Available online at www.scholarsresearchlibrary.com

Scholars Research Library

European Journal of Applied Engineering and Scientific Research, 2017, 5(1): 14-27

ISSN: 2278-0041

The Electrical Switching Properties of $Ge_{10}Se_5Sb_{85}$ Chalcogenide Glass

S Abouelhassan*

Physics Department, Faculty of Science, Jazan University, KSA

ABSTRACT

Bulk ingot material of the ternary mixture $Ge_{10}Se_5Sb_{85}$ was prepared by direct fusion of high purity constituent elements in vacuum sealed silica tube. The glassy nature of the prepared sample was confirmed by the X-ray diffraction (XRD) technique. Current -Voltage characteristics of the investigated glass have been carried out at different thicknesses and temperatures. Switching phenomenon at the turn-over point (TOP) from a high-resistance state (OFF state) to a negative-differential resistance-state (NDRS) was detected where the threshold parameters such as threshold dissipated power (P_{th}) ,threshold voltage(V_{th}),threshold current (I_{th}),threshold electric field (E_{th}) and threshold resistance (R_{th})were determined at different thicknesses and ambient temperatures of the investigated samples. At the turn-over point ,the activation energies $\left(\Delta E_p, \Delta E_v, \Delta E_i, \Delta E_r \text{and } \Delta E_f\right)$ *caused by the threshold dissipated powers, threshold voltages, threshold currents, threshold resistances and threshold electric fields respectively, were deduced at different thicknesses of the samples. The increasing in the ambient temperature of the investigated material (ΔT_J), the temperature of the conduction path ($T^{\prime}$) and the Poole-Frenkel coefficient (β_{PF}) were determined at different ambient temperatures and thicknesses of the samples on the basis of the Joule heating effects. The activation energy of hopping (W), the activation energy of conduction ΔE_σ(eV), the hopping distance (d) of the charge carriers and the density of localized states N(E) were carried out due to Poole-Frenkel effect.*

Keywords: Switching, Chalcogenide, Glass, Poole-Frenkel effect

---

INTRODUCTION

One of the most important classes of glass is the chalcogenide glass. It contains at least one of the chalcogen elements; sulfur, selenium or tellurium, and is of essential interest owing to their wide application in optoelectronics, electrical and optical memory devices, modern electronics, and solar cells. Chalcogenide glass has attracted great attention because of their interesting semiconducting properties [1,2] that can be used in various solid state-devices, such as power control and information storage devices and also because of their more recent importance in optical recording [3]. They are considered as core materials for optical fibers for light transmission, particularly when small lengths and flexibility are required. Binary and ternary chalcogenide glasses exhibit many useful properties including, particularly, the switching phenomenon. In chalcogenide glass there exists two types of switching which are threshold and memory switching based on the way the glasses respond to the removal of the electric field after the switching event [4-12]. In the first type of switching, the ON state can be observed only when a current flows down to a certain holding voltage, while in the memory type one, the ON state is permanent until a suitable reset current pulse is applied on the sample [13]. The

investigated glasses are important due to their interesting optical properties for their potential use as optical fibers, and electrical memory devices. The phenomenon of electrical switching in this type of glass has attracted several technological applications including power control and information storage.

In threshold-type switching, no structural changes occur and the process could be considered as reversible, whereas in memory-type switching, the material undergoes significant structural changes after transition and the process becomes completely irreversible [14,15]. The sudden change in the electrical resistance of chalcogenide glasses from a low conducting "OFF" state to a high conducting "ON" state under the effect of an appropriate electric field is commonly referred to as the switching/threshold electric field [16]. The switching process consists of a change of several orders of magnitude in electrical resistance caused by the application of a voltage higher than a critical voltage known as the threshold or switching voltage(v_{th}), which corresponds to the threshold resistance (R_{th}), threshold current (I_{th}), threshold dissipated power (P_{th}) , and threshold electric field (E_{th}). The application of a high electric field across high-resistivity materials sometimes results in either switching to a low-resistance state or entering a region of current- controlled negative resistance (CCNR) [17]. On the removal of the excitation electric field, threshold switching glasses revert to the OFF state whereas memory switches remain locked to the ON state [18]. Memory switches originate from the boundaries of the glass-forming regions, where glasses tend to crystallize when heated or cooled slowly [19-21]. There are several models proposed to understand the memory and threshold types of electrical switching, which are exhibited by the chalcogenide glasses. They have been classified into purely electronic [22], thermal and electrothermal models [23-27]. The electronic mechanism appears to govern thin films, while the electrothermal model appears to control the bulk specimens [28] and some investigators [23,29,30] have considered the threshold switching as an electronic process. Investigations on the current-voltage characteristics and some studies on the dependence of the switching voltage and current on different material properties, such as composition, thickness, and pressure, will help investigators to understand the conduction mechanisms of the chalcogenide glasses. In the present work, the effect of thickness and temperature on the I-V characteristics and some switching parameters of $Ge_{10}Se_5Sb_{85}$ chalcogenide glasses will be investigate

MATERIALS AND METHODS

Bulk chalcogenide glasses of $Ge_{10}Se_5Sb_{85}$ were prepared using the conventional melt quenching technique. Elemental constituents of 5N purity were weighed according to their atomic percentages and sealed in evacuated (10-5 Torr) silica tubes then heated gradually to 1223 K for 15 h. The melt was continuously stirred to ensure homogeneity and then rapidly quenched in ice water. The glassy nature of the prepared samples was confirmed by the X-ray diffraction (XRD) technique using a Shimadzu XD-3 diffractometer with scanning velocity of 20 scans/min and Cu foil as the radiation source. Current–voltage characteristics were analyzed point by point using two electrometers (Keithley 617C). The glass samples were sandwiched between two electrodes, one of which was a pin electrode. The best fit for the resultant data points was made using the least-square method.

RESULTS AND DISCUSSION

Temperature dependence of the I-V characteristics of $Ge_{10}Se_5Sb_{85}$

Current-voltage (I-V) characteristics and switching phenomena of different thicknesses of amorphous $Ge_{10}Se_5Sb_{85}$ at different ambient temperatures are given in Figures1a-1d. From the figures it can be noticed that the sample exhibit an Ohmic behavior at lower applied voltages which is characterized by the high resistance state (OFFstate).

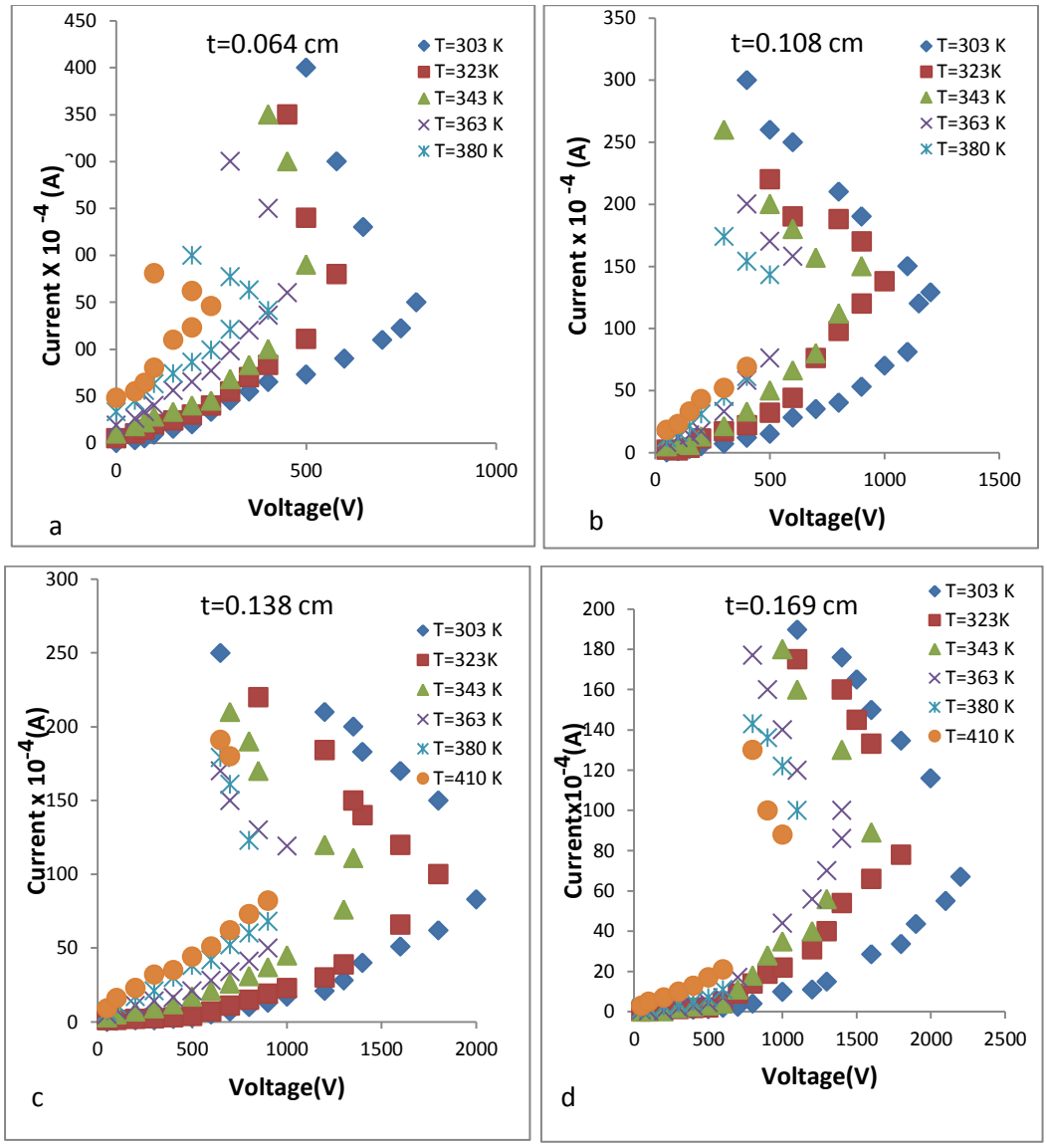

Figure 1: The I-V characteristics of different thicknesses (t=0.064 cm, t=0.108 cm, t=0.138 cm and t=0.169 cm) for the glassy sample Ge_5Se_{15} Sb_{85} at different ambient temperatures

The OFF state region ,for the investigated samples(t=0.064 cm as a representative sample) can be redrawn, as shown in Figures 2a-2d, where it can be observed that, as the voltage across the sample increases , then the current increase linearly (Ohmic behavior), forming the first region (o-a) in the OFF state, which represents the high-resistance state.

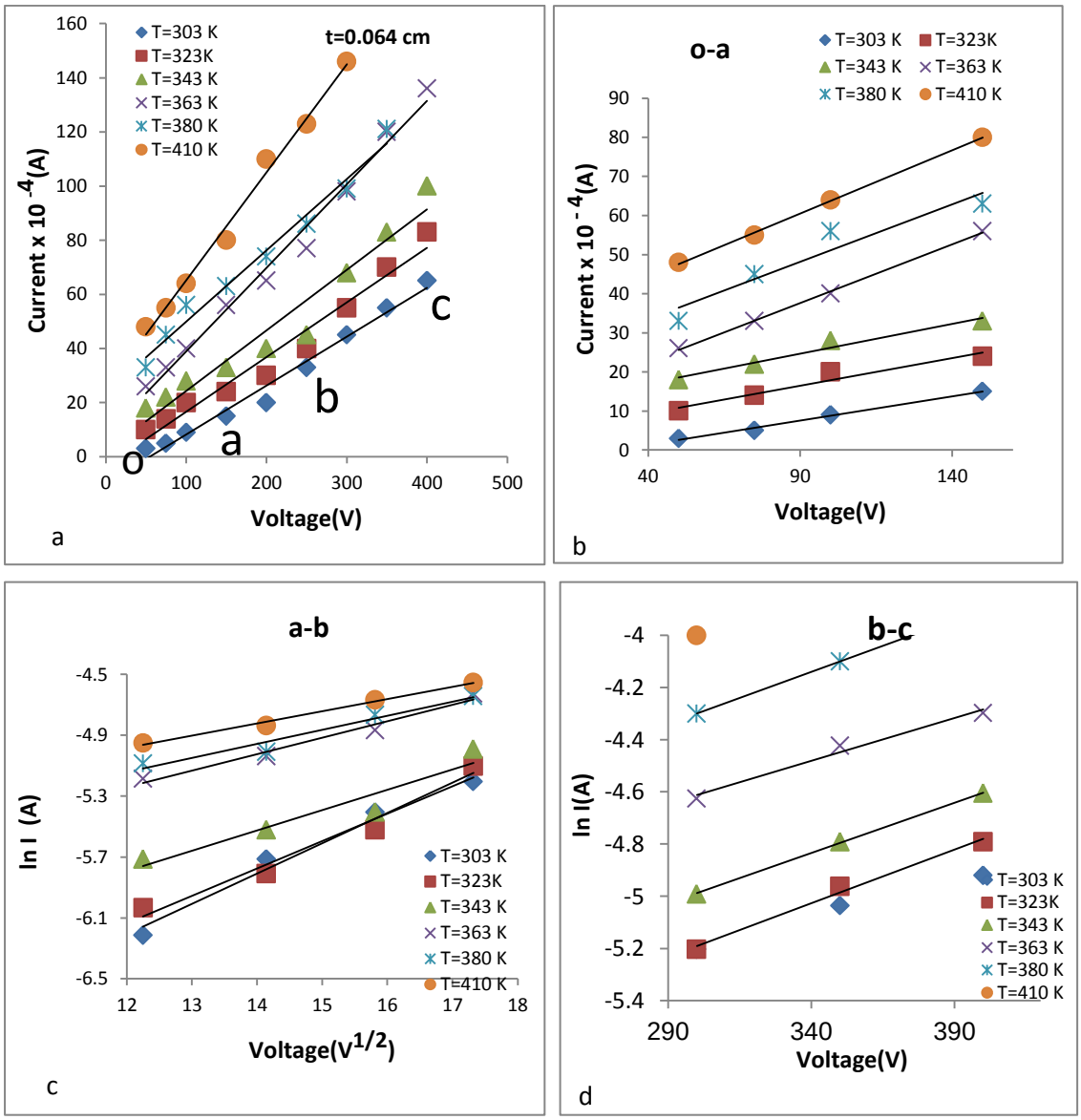

Figure 2: The I-V characteristics of the sample (t=0.064 cm) at different ambient temperatures in the OFF state

The dc conductivity of the investigated samples was plotted (Figure 3) against the ambient temperature, at different thickness, according to the relation:

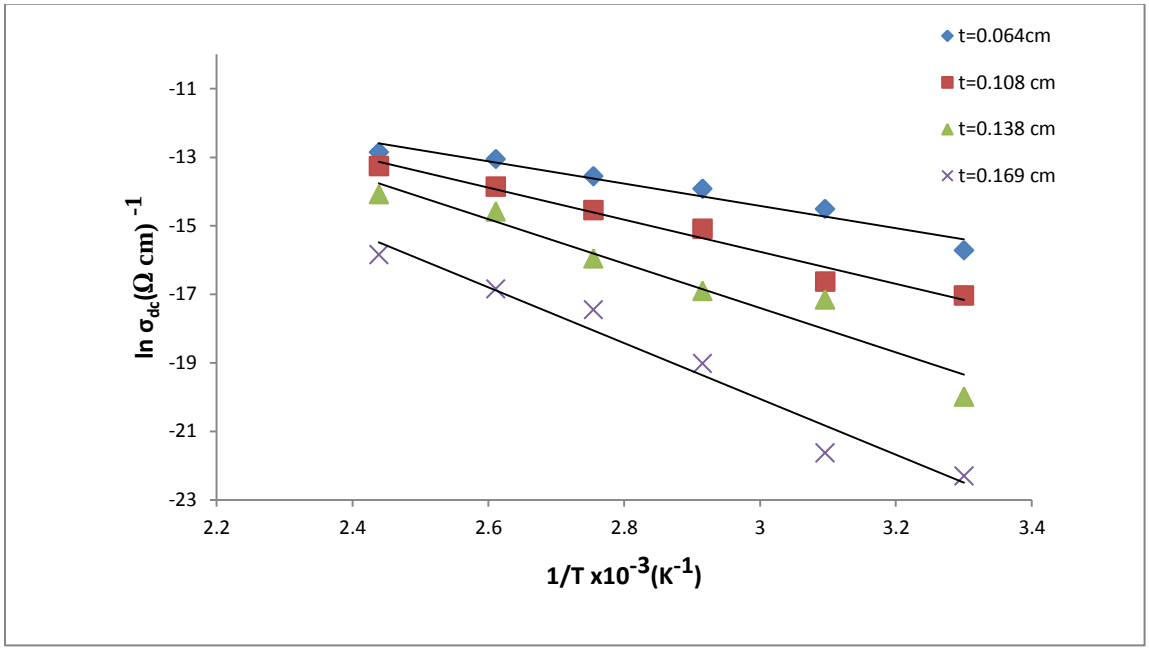

Figure 3: The temperature dependence of the dc conductivity of Ge_{10} Se_5 Sb_{85} at different ambient temperatures

$$\sigma_{dc} = \sigma_o \exp\left(-\Delta E_\sigma / k_B T\right)$$

Where ΔE_σ is the activation energy of conduction. The deduced values of ΔE_σ at different thickness of the investigated samples are given in Table 1 where it can be noticed that as the sample thickness increases, the conductivity decreases which may be attributed to the increase in the disorder scattering process of the charge carriers which leads to increase the activation energy of conduction with the sample thickness as given in Table 2 and Figures 3-9.

Table 1: The obtained values of the density of states $N(E_F)$, hopping distance (d) and hopping energy W(eV) at different temperatures and thicknesses of $Ge_{10}Se_5Sb_{85}$

	t=0.064 cm			t=0.108 cm			t=0.138 cm			t=0.169 cm		
Temperature (K)	$N(E_F)$ (10^{15} eV^{-1} cm^{-3})	**d (10^{-6} m)**	W(eV)	$N(E_F)$ (10^{16} eV^{-1} cm^{-3})	**d (10^{-6}cm)**	W(eV)	$N(E_F)$ (10^{16} eV^{-1} cm^{-3})	**d (10^{-6} cm)**	W(eV)	$N(E_F)$ (10^{16} eV^{-1} cm^{-3})	**d (10^{-6} cm)**	W(eV)
303	0.78	6.46	1.126	4.2	4.23	0.737	10.9	3.34	0.582	14.5	3.11	0.543
323	2.99	4.55	0.845	8.5	4.10	0.762	11.7	3.23	0.601	16.2	2.98	0.554
343	12.01	3.16	0.774	13.0	3.92	0.674	14.0	3.04	0.581	19.2	2.81	0.555
363	34.66	2.18	0.655	36.1	2.40	0.602	38.4	2.64	0.551	39.6	2.53	0.529

380	45.89	0.189	0.456	51.4	.016	0.429	47.5	0.002	o.390	52.87	.00013	0.34
410	90.72	0.003	0.290	78.6	0.002	0.138	88.34	0.001	0.108	92.09	0.0005	0.0163

The region o-a is followed by a second one (a-b), which exhibits exponential behavior verifying the relation [31-33]:

$$I = I_o \exp\left(V / V_o\right)^{1/2}$$

Where I_o is the potential difference across the sample, $V_o = 4k_B{}^2T^2t / \beta_{PF}$, with k_B being the Boltzmann constant, T is the ambient temperature of the sample, t is the sample thickness, and β_{PF} is the Poole-Frenkel coefficient. The relationship between ln I and $V^{\frac{1}{2}}$ at different constant ambient temperatures for the sample t = 0.064 cm is shown in Figures 2a-2b, where β_{PF} is determined and given in Table 1.

From this table it can be observed that β_{PF} tends to decrease as the ambient temperature increases, while it exhibits increasing behavior as the sample thickness increases which indicates that the conduction mechanism in the (a-b) region of the OFF state follows either the Schottky emission [34] or the Poole-Frenkel- type conduction [35]. The region (b-c) in the OFF state seems to be linear as shown in Figures 2b and 2c.

The samples exhibit a sudden change from a high- resistance (OFF) state to a negative-differential-resistance state (NDRS). The point at which the curves switch from the OFF state to the NDRS is called the turn-over point (TOP).

Table 2: The obtained values of the RISE in the ambient temperature of the material (ΔT_J), temperature of the conduction path ($T^{\backslash}$) and the Poole - Frenkel coefficient (β_{PF}) at different temperatures and thicknesses of $Ge_{10}Se_5Sb_{85}$

	t=0.064 cm			t=0.108 cm			t=0.138 cm			t=0.169 cm		
Temperature (K)	**ΔT_J (K)**	$T^{\backslash}$ **(K)**	**β_{PF} x10^{-8}**	**ΔT_J (K)**	$T^{\backslash}$ **(K)**	**β_{PF} x10^{-8}**	**ΔT_J (K)**	$T^{\backslash}$ **(K)**	**β_{PF} x10^{-8}**	**ΔT_J (K)**	$T^{\backslash}$ **(K)**	**β_{PF} x10^{-8}**
303	19.8	322.8	6.42	16.7	319.7	6.77	13.9	316.9	7.01	10.1	313.1	7.4

323	22.3	345.3	4.59	21.5	344.5	6.68	15.8	338.8	6.90	11.5	334.5	7.2
343	24.1	367.1	3.24	23.5	366.5	6.48	17.9	360.9	6.6	13.0	356.	6.9
363	27.9	390.9	2.26	25.7	388.7	4.03	20.1	383.1	5.80	14.6	377.6	6.3
380	29.8	409.8	1.82	27.3	407.3	3.31	25.7	405.7	4.20	17.9	397.9	5.1
410	32.54	433.5	1.13	29.94	439.9	2.17	28.4	438.4	3.45	20.1	430.1	4.37

The switching behavior is accompanied by the burning or heating of the conduction path which in turn may lead to the Joule heating effect during the initial stage of switching because of the high resistance of the samples that leads to an increase in the conduction path temperature ($T^{\backslash}$). This temperature was calculated for different thicknesses of the samples at constant ambient temperatures according to the relation [36,37]:

$$T^{\backslash} = T + \Delta T_J$$

Where T is the ambient temperature and ΔT_J is the increase in the temperature of the conduction path, which is given by:

$$\Delta T_J = kT^2 / [\Delta E_\sigma - kT]$$

Where ΔE_σ is the activation energy of conduction and k is the Boltzmann constant. The calculated values of $T^{\backslash}$ and ΔT_J are given in Table 1, where it can be observed that as the ambient temperature increases, the temperature of the conduction path $T^{\backslash}$ increases consequently, ΔT_J increases, which enhances the proposed concept of the Joule heating effect and is in agreement with previously reported results [37-40]. The parameters related to the TOP, such as the threshold voltage V_{th} , threshold current I_{th} , threshold resistance R_{th} and threshold power P_{th} ,are calculated and their dependences on the sample thickness and temperature are discussed below.

Temperature dependence of the threshold voltage of $Ge_{10}Se_5Sb_{85}$

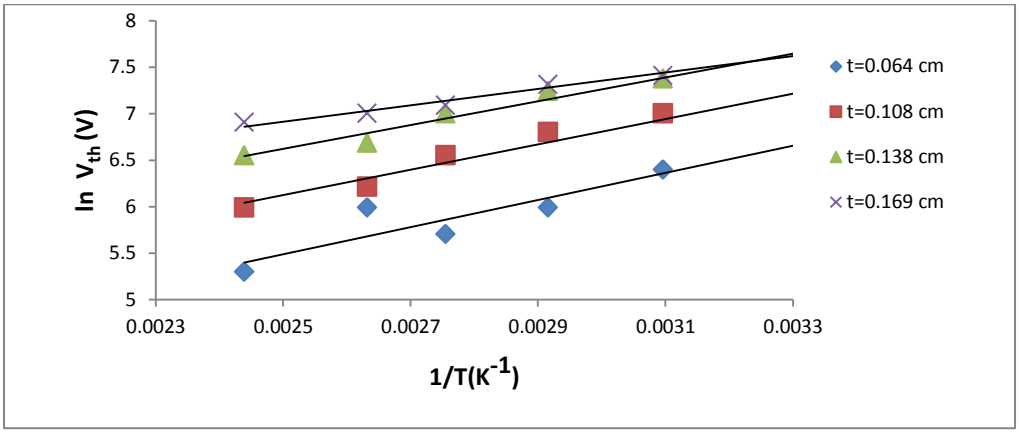

Figure 4: The temperature dependence of the threshold voltage at constant thickness of the sample

The temperature dependence of the threshold voltage (V_{th}) at different thicknesses for the sample $Ge_{10}Se_5Sb_{85}$ is shown in Figure 4 where an increase in V_{th} as the ambient temperature increases is observed, verifying the relation [38]:

$$V_{th} = V_o \exp\left(\Delta E_v / kT\right)$$

Where V_o is a temperature-independent parameter and ΔE_v is the threshold voltage activation energy related to the temperature of the conduction path. The linear plots between ln (V_{th}) and (1/T) can be understood [37,39] in terms of the electrothermal model for the pre-switching region as follows: The temperature dependence of the threshold voltage is an important factor that characterizes the robustness of the material against thermal degradation and hence the stability of the material for device applications [41]. The memory switching in chalcogenide glasses involves the formation of a conducting crystalline filament in the material, and hence a decrease in threshold voltage is expected [42]. Most amorphous materials contain dipoles dispersed randomly through the amorphous matrix. As an electric field is applied, these dipoles tend to orient in the direction of this field. The orientation process depends on the viscosity of the amorphous matrix as well as on the applied electric field. As the temperature of the conduction path increases, its viscosity decreases, enhancing the orientation process, up to the TOP. At this point, the resultant force of the resistance for dipole orientation in a viscous amorphous medium diminishes therefore, the switching process take occurs. Thus, as the ambient temperature increases, the viscosity of the conduction path decreases, therefore the field's ability to cause a maximum dipole orientation should decrease [37,39].

The thickness dependence of the threshold voltage for the investigated sample can be observed in Figure 4, where an increase in V_{th} with the sample thickness is obtained. It has been suggested earlier [43] that V_{th} varies with t, $t^{1/2}$, or t^2 depending on whether the mechanism responsible for switching is electronic, purely thermal, or electrothermal respectively. The results indicate the presence of electrothermal processes operating during the progress of the crystallization mechanism in the conduction path. It has been considered that as the

sample thickness increases, the dissipated power inside the conduction path increases, which leads to an increase in the required field, consequently the threshold voltage increases, which is in agreement with previously reported results [44-46]. The values of ΔE_v at different thicknesses were deduced using the least-squares fitting method and are given in Figure 9. From this figure it can be observed that ΔE_v decreases as the thickness increases. The decrease in ΔE_v may be interpreted in terms of the localized state concept, which is calculated according to the relation [47]:

$$\beta_{PF} = \left[\frac{64\alpha^4 t^4}{\pi\, e\, N(E_F)} \right]^{1/4}$$

Where α^{-1} is the radius of the electron wave function, t is the sample thickness, and $N(E_F)$ is the density of localized states at the Fermi level. The calculated values of $N(E_F)$ are given in Table 2, where it can be observed that $N(E_F)$ tends to increase as the sample thickness increases, which results in a decrease in the hopping distance of the charge carriers between the filled and empty states. The calculated values of the hopping distance (d), according to the relation [48-50]: $d = \left[9 / \left(8\, N(E_F)\, \pi\, \alpha\, k\, T \right) \right]^{1/4}$, are given in Table 2 where it can be noted that a decrease in d consequently results in a decrease in the required average hopping energy $W(eV)$ between the filled and empty states. The calculated values of $W(eV)$ according to the relation [50]: $W(eV) = \left[3 / \left(4\pi\, d^3 N(E_F) \right) \right]$ are given in Table 2.

Temperature dependence of the threshold current of $Ge_{10}Se_5Sb_{85}$

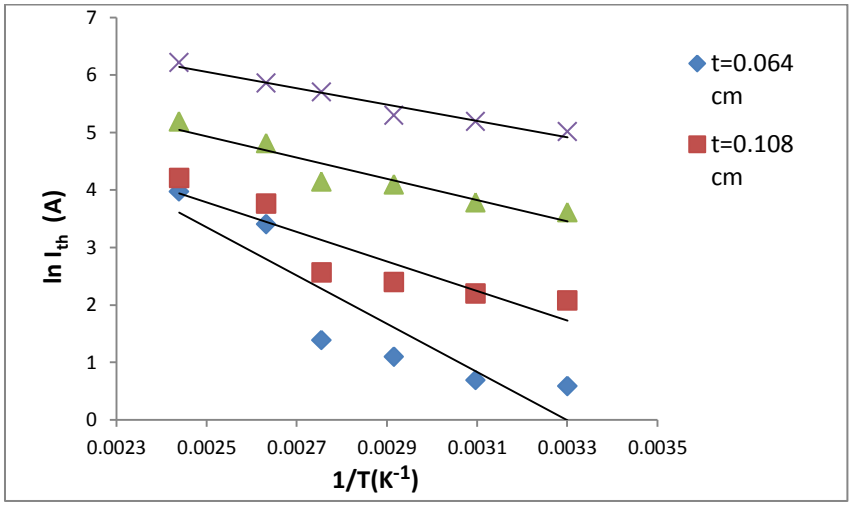

Figure 5: The temperature dependence of the threshold current at constant thickness of the sample

Figure 5 shows the temperature dependence of the threshold current I_{th} for the investigated sample, which yields straight lines obeying the equation 38:

$$I_{th} = I_o \exp\left(-\Delta E_i / kT \right)$$

Where Io is an independent term and ΔE_i is the activation energy term related to the conduction mechanism. From this figure, it can be noticed that as the ambient temperature increases the threshold current increases, which may be attributed to an increase in the area of the conduction path where the crystallization process is enhanced. The deduced values of ΔE_i at different thicknesses are given in Figure 9. It can be observed that as the sample thickness increases, ΔE_i tends to decrease. The decreasing behaviour may be attributed to the increased area of the conduction path.

Temperature dependence of the threshold resistance of $Ge_{10}Se_5Sb_{85}$

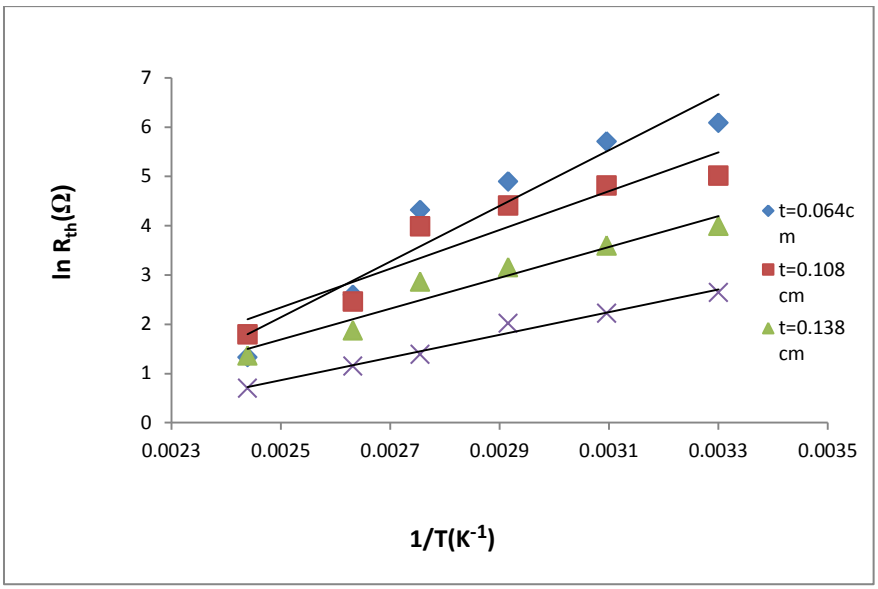

Figure 6: The temperature dependence of the threshold resistance at constant thickness of the sample

Figure 6 shows the temperature dependence of the threshold resistance R_{th} for the investigated sample, which yields straight lines obeying the equation [38]:

$$R_{th} = R_o \exp\left(\Delta E_r / kT\right)$$

Where R_o is an independent term and ΔE_r is the activation energy term related to the conduction mechanism. It is observed that as the ambient temperature increases, the threshold resistance decreases. The threshold resistance increase as as the thickness of the sample increases. This may be attributed to an increase in the conduction path area. The values of ΔE_r were deduced for different thicknesses of the investigated sample using the least- squares fitting method and are given in Figure 9.

From this figure it can be observed that ΔE_r tends to decreases gradually with the sample thickness, which is in agreement with previously reported results [37-46].

Temperature dependence of the threshold dissipated power of $Ge_{10}Se_5Sb_{85}$

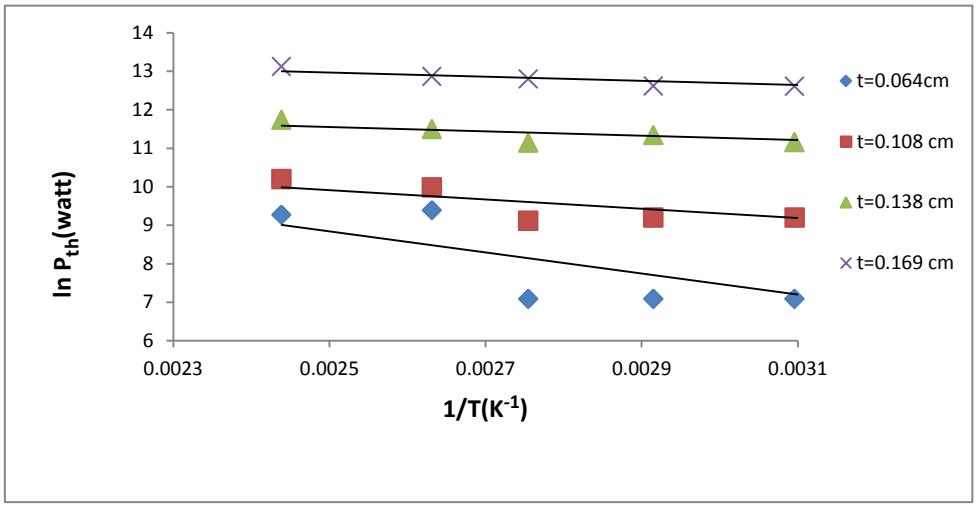

Figure 7: The temperature dependence of the threshold power at constant thickness of the sample

The threshold dissipated power P_{th} $\left(P_{th} = V_{th} I_{th}\right)$ in the conduction path of the sample at the threshold voltage was calculated at different thicknesses of the investigated sample and is plotted (Figure 7) as ln P_{th} against 1/T according to the relation [38] :

$$P_{th} = P_o \exp\left(-\Delta E_p / kT\right)$$

Where ΔE_p is the activation energy at the threshold power. From Figure 7 it can be observed that P_{th} decreases as the temperature increases. This may be due to the decrease in the number of collisions between the charge carriers in the samples. The values of ΔE_p were deduced and plotted as given in Figure 9 at different thicknesses of the investigated samples. It can be observed that ΔE_p decreases as the sample thickness increases which may be attributed to the deterioration of the scattering process between the charge carriers as a result of the enhanced process in the crystallization mechanism at the threshold point.

Temperature dependence of the threshold Electric field of $Ge_{10}Se_5Sb_{85}$

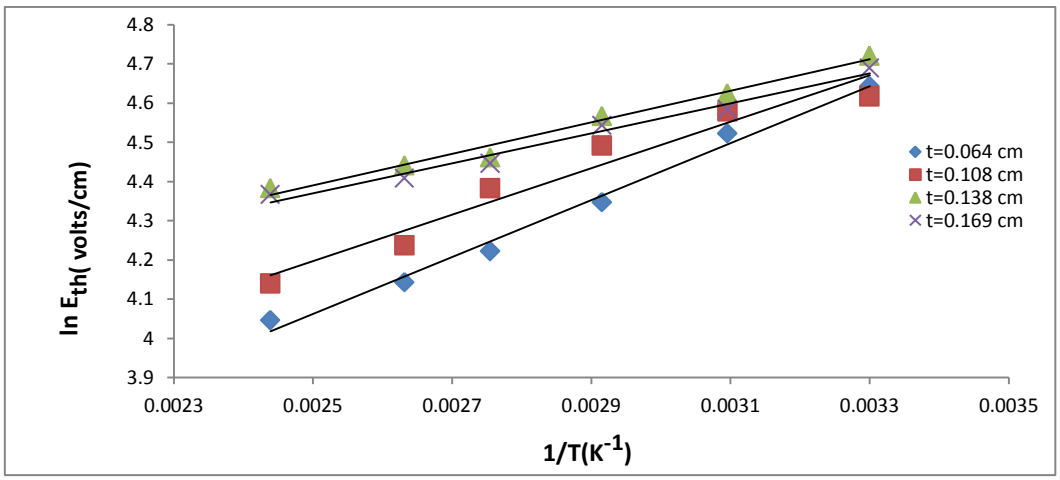

Figure 8: The temperature dependence of the threshold electric field (Eth) of Ge_5Se_{15} Sb_{85}

The threshold Electric field $E_{th}\left(V_{th} = t\right)$ in the conduction path of the sample at the (TOP) was calculated at different thicknesses of the investigated sample and is plotted (Figure 8) as ln E_{th} against 1/T obeying the relation,

$$E_{th} = E_o \exp\left(\Delta E_f / kT\right)$$

Where ΔE_f is the activation energy at the (TOP). From Figure 8 it can be noticed that as the temperature of the sample increases, the threshold electric field decrease. The deduced values of ΔE_f are plotted against the sample thickness as given in Figure 9. It can be noticed that as the sample thickness increases, ΔE_f decrease which may be attributed to the increasing in the orientation process of the dipoles in the direction of the applied electric field**.**

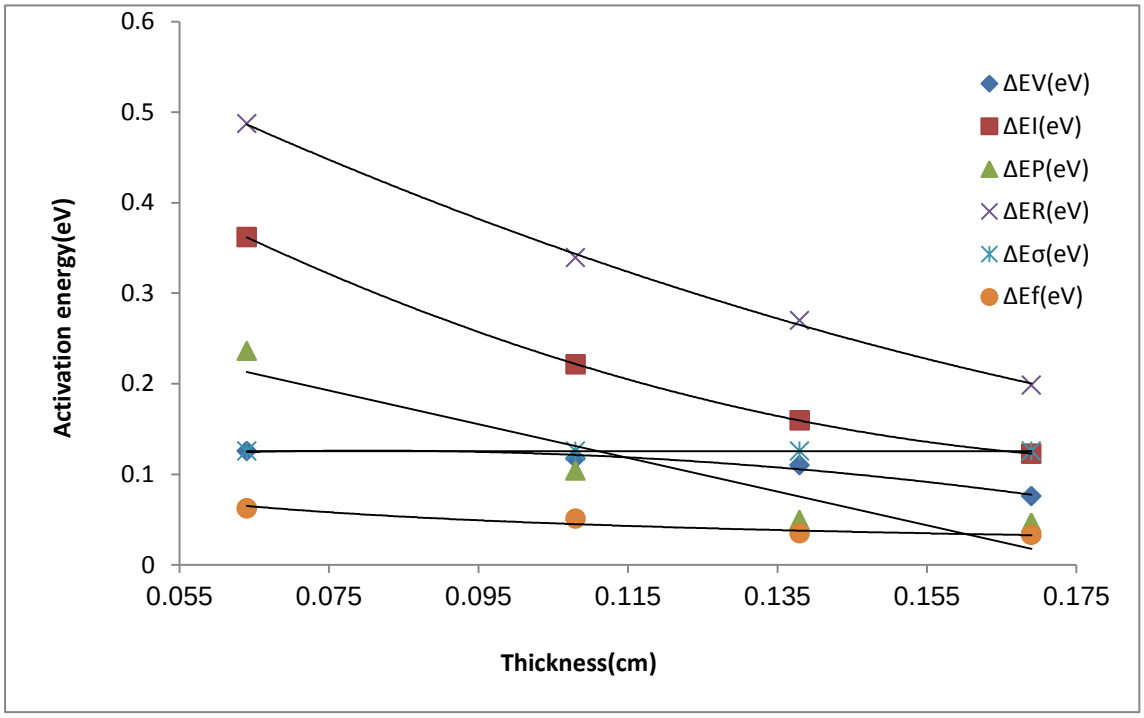

Figure 9: The thickness dependence of the activation energy of Ge10Se5 Sb85

CONCLUSION

Bulk chalcogenide glasses of Ge10Se5Sb85 were prepared using the conventional melt quenching technique. The glassy nature of the prepared samples was confirmed by the X-ray diffraction technique. Switching phenomenon at the turn-over point (TOP) from a high-resistance state (OFF state) to a negative-differential resistance-state (NDRS) was detected where the threshold parameters such as threshold dissipated power (P_{th}) ,threshold voltage(V_{th}),threshold current (I_{th}),threshold electric field (E_{th}) and threshold resistance(R_{th})were determined at different thicknesses and ambient temperatures of the investigated samples. The activation energies of the investigated samples (ΔE_p , ΔE_v , ΔE_i , ΔE_r and ΔE_f) ,at the turn-over point,indicate a decreasing behavior with the sample thickness. The obtained values of the rise in the ambient temperature of the material (ΔT_J), temperature of the conduction path $(T^{\backslash})$ and the Poole - Frenkel coefficient (β_{PF}) at different temperatures and thicknesses were explained in terms of Poole-Frenkel effect.

Acknowledgment

The author would like to express his deep thanks to Jazan University for its financial support.

REFERENCES

[1] Tanaka, K., et al., *Journal of Non-Crystalline Solids*, **1973.** 12: p. 100.

[2] Shaabam, E.R., *Physica B*, **2006.** 373: p.211.

[3] Sugiyama, Y., et al., *Journal of Non-Crystalline Solids*, **1990.** 83.

[4] Ovshinsky, S.R., and Frizsche, H., *Metallurgical and Materials Transactions*, **1971.** 2641.

[5] Adler, D., *Scientific American*, **1977.** 236: p.36.

[6] Davis, E.A. and Mott, N.F., *Electronic Processes in Non-Crystalline Materials*, **1979**.

[7] Sarkar, D., Sanjeev, G, and Mahesha, M.G., *Applied physics A*, **2015.** 119: p. 49.

[8] Karuppaprnao, R., Ganesan, V, and Asokan, S., *International Journal of Applied glass science*, **2011.** 2(1): p. 52.

[9] Sreevidya, G., et al., *Journal of Applied Physics*, **2014.** 115: p. 164505.

[10] Malligavathy, M., *Journal of Non-Crystalline Solids*, **2015.** 429: p. 93.

[11] Chandasree, D., Mohan Rao, G, and Asokan, S., *Materials Research Bulletin*, **2014.** 49: p.388.

[12] Kumari, V., et al., *Proceeding and Application of Ceramics*, **2015.** 9(1): p. 61.

[13] 10th International conference on development and application systems, Suceava Romania, **2010**.

[14] Platakis, N.S., *Journal of Non-crystalline Solids*, **1978.** 27**:** p. 331.

[15] Mio, A.M., *Journal of Applied physics*, **2015.** 18: p. 064503.

[16] Ovshinsky, S.R., *Physical Review Letters*, **1968.** 21: p. 1450.

[17] Soltan, A.S. and Moharram, A.H., *Physica B*, **2004.** 349: p. 92.

[18] Pattanayak, P. and Asokan, S., *Solid State communications*, **2007.** 142**:** p. 698.

[19] Savage, J.A., *Journal of Material Science*, **1972.** 7: p. 64.

[20] Cornet, J., *Ann Chem*, **1975.** 10: p. 239.

[21] Moss, C. and Deneufville, J.P., *Materials Research Bulletin*, **1972.** 79**:** p. 423.

[22] Owen, A.E. and Robertson, J.M., *IEEE Transactions on Electronic Devices*, **1973.** 20**:** p.105.

[23] Klein, N., *Thin Solid Films*, **1971.** 7: p. 149.

[24] Adler, A., et al., *Journal of Applied Physics Letters*, **1973.** 22: p.114.

[25] Kaplan, T. and Adler, D., *Journal of Applied Physics Letters*, **1971.** 19: p. 418.

[26] Kroll, D.M., *Physical Review B*, **1974.** 9**:** p. 1669.

[27] Madhu, B.J., Jayanna, H.S, and Asokan, S., *Journal of Non-Crystalline Solids*, **2009.** 355**:** p. 459.

[28] Alegria, A., Arrubarrena, A, and Sanz, F., *Journal of Non-Crystalline Solids*, **1983.** 58: p. 17.

[29] Vezzoli, G.C., Walsh, P.J, and Doremus, L.W., *Journal of Non-Crystalline Solids*, **1975.** 18: p. 333.

[30] Devaraju, J.T., *Philosophical Magazine part B*, **2001.**81: p. 583.

[31] Burgelman, M., *Solid State Electronics*, **1977.** 20: p. 523.

[32] Denton, G.A., Friedman, G.M, and Schetzina, *Journal of Applied Physics*, **1957.** 46**:** p. 3004.

[33] Abdel-Aziz, M.M., *Applied Surface Science*, **2006.** 253**:** p. 2059.

[34] Jonsher, A.K., *Thin Solid Films*, **1967.** 1**:** p. 213.

[35] Dwyer, J.J.O., The theory of Electrical Conduction and Breakdown in Solid Dielectrics, Clarendon Press, Oxford, **1979.** p.220.

[36] Abouelhassan S., Thesis, Benha Uni., Faculty of science, **1987**.

[37] El-Mansy, M.K., et al., *Applied Physics Communication*, **1994.** 13: p. 187.

[38] Nakashima, K. and Kao, K., *Journal of Non-Crystalline Solids*, **1979.** 33: p. 189.

[39] Abouelhassan, S. and Khoder, H., *physica status solidi (a)*, **2001.** 186: p. 401.

[40] Roy, D., et al., *International Journal of Chemical, Molecular, Nuclear, Material and Metallurgical engineering*, **2016.** 10(6**)**: p. 604**.**

[41] Ovshinsky, S.R. and Frizsche, H., *IEEE Transactions on Electron Devices***, 1973.** 20(2): p. 91.

[42] Lokesh, R., Udyashankar, N.K, and Asokan, S., *Journal of Non-crystalline Solids*, **2010**. 356: p. 321.

[43] Jones, G. and Collins, R.A., *physica status solidi*, **1979.** 53**:** p. 339.

[44] Mansour, E., et al., *Physica B*, **2001.** 305**:** p. 242.

[45] Gouda, M., Khodair, H, and El-shaarawy, M.G., *Materials chemistry and physics*, **2010.** 120: p. 608.

[46] Hench, L.L., *Journal of Non-Crystalline Solids*, **2009.** 2: p. 250.

[47] Mott, N.F. and Davis, E.A., *Electronic Processes in Non-Crystalline Materials*, Clarendon, Oxford, **1971.**

[48] Mott, N.F., *Philosophical Magazine*, **1969.** 19**:** p. 835.

[49] Elliott, S.R., *Physics of Amorphous Materials*, **1984.**

[50] Hill, R.M., *Philosophical Magazine*, **1971.** 24**:** p. 1307.